1

Basic Principles of Photocatalysis

Baker Rhimi and Zhifeng Jiang

Jiangsu University, Institute for Energy Research, School of Chemistry and Chemical Engineering, Zhenjiang 212013, China

1.1 Introduction

Solar energy, being the primary energy source derived from extraterrestrial space, represents a boundless and renewable resource with the potential to surpass global energy demands. Solar energy is widely regarded as the ultimate renewable resource available on Earth due to the long-predicted lifetime of the sun. However, the energy source under consideration poses notable challenges in terms of harvesting, storage, and utilization due to its diurnal and intermittent features [1, 2]. Currently, there exist various technologies that can be employed to tackle these challenges. One avenue of exploration involves collecting and converting solar energy into thermal energy, which can be utilized to provide heat to residential areas or be further transformed into electricity, along with other types of energy. One of the most extensively researched areas in solar photon harvesting pertains to technologies based on the photovoltaic effect, which relies on advancements in semiconductor theory and practice. These advancements have greatly propelled the field, enabling the efficient transformation of sunlight into electrical energy.

Photochemical reactions are another well-studied approach for the harvesting and storage of solar energy. The underlying reason is that chemical bonds serve as advantageous mediums for the storage of energy. Over billions of years, biological sources, primarily through photosynthesis, have contributed to the composition of the Earth's atmosphere, with oxygen (O_2) constituting approximately 21% of its makeup. This cumulative energy derived from chemical reactions throughout evolutionary history is of immense magnitude, surpassing the quantifiable extent of known reserves of fossil fuels. The understanding of natural photosynthesis process has served as a source of inspiration for numerous scientists, motivating them to create technologies that surpass their efficiency and cost-effectiveness in order to address our continuously expanding energy demands. Nevertheless, it is

Layered Materials in Photocatalysis: Environmental Purification and Energy Conversion, First Edition. Edited by Liqun Ye and Dehua Xia.

crucial to realize that the full investigation of photosynthesis extends beyond the field of solar energy storage, yielding wider implications. The utilization of photon energy, rather than heat to facilitate and potentially drive chemical reactions is a topic of considerable academic interest. The field of study encompassing this particular area of research has been widely recognized and commonly referred to as photocatalysis [3].

Photocatalysis has emerged as a promising approach to tackle environmental and energy challenges by harnessing solar radiation, and it has received significant global interest over the past five decades [4–6]. Research interest in photocatalysis has grown due to the increasing emphasis on sustainability. One promising application of photocatalysis is the direct storage of solar energy in chemicals, also known as solar fuels and artificial photosynthesis. This chapter starts by elucidating the fundamental principles underlying the interaction between light and matter, as well as the electronic structure of semiconductors. These concepts serve as the basis for understanding photocatalysis. Furthermore, this chapter explores the key steps of charge generation, separation, and transfer that take place within photocatalytic systems. The mechanisms by which photon-induced electron–hole pairs are formed, dissociated, and directed toward specific chemical reactions are explored. Special attention is given to the factors influencing photocatalytic performance, including the selection of appropriate materials, surface modifications, and cocatalyst strategies. The role of dopants, facet engineering, and heterojunctions in enhancing photocatalytic performance is discussed, shedding light on the strategies employed to improve the overall efficiency of photocatalytic systems. Finally, the chapter highlights some key applications of photocatalysis, such as solar hydrogen production through photocatalytic water splitting and environmental remediation by providing real-world examples and case studies.

1.2 Definition and Fundamental Principles of Photocatalysis

Photocatalysis, which takes inspiration from natural photosynthesis, involves the use of light to drive fundamental processes [7, 8]. Photosynthesis is the term used to describe the mechanism through which green plants, microalgae, and certain bacteria capture sunlight energy to drive energetically demanding reactions, such as the conversion of carbon dioxide (CO_2) and water (H_2O) into carbohydrates. While the specific mechanisms of photosynthesis can differ among various organisms, they are grounded in fundamental principles that are shared. The general framework of oxygenic photosynthesis, depicted in Figure 1.1a, serves as a basis for understanding these processes. This process, known as the "Z-scheme," involves two photosystems (PSI and PSII) as the key components. In PSII, chlorophylls absorb photons with a maximum wavelength of 680 nm (P680) and transfer the energy to extract electrons from H_2O, resulting in the production of oxygen through water-oxidation catalysts. The separated electrons are then transferred to PSI, where chlorophylls absorb

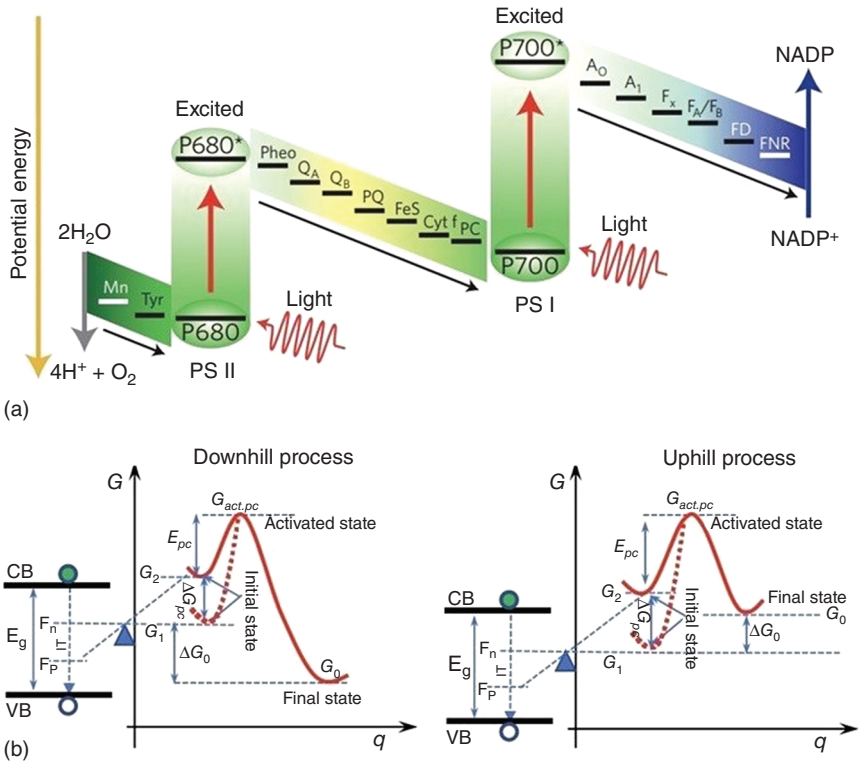

Figure 1.1 (a) Schematic representation of natural photosynthesis. Source: Reproduced with permission from Tachibana et al. [9]/Springer Nature. (b) Gibbs free energy landscape (*G*-potential landscape) of downhill and uphill photocatalytic reactions via the interfacial electron transfer (IET). Source: Reproduced with permission from Liu et al. [10]/American Chemical Society.

photons with a maximum wavelength of 700 nm (P700). The energy from these photons further excites the electrons transferred from PSII, enabling them to reduce nicotinamide adenine dinucleotide phosphate ($NADP^+ \rightarrow NADPH$). Along with the proton gradient generated during the process, NADPH drives downstream transformations, such as the conversion of CO_2 to hydrocarbons via the Calvin cycle [7, 9]. The key aspect of natural photosynthesis is its ability to drive chemical reactions using optical energy. Photocatalysis, which dates back to early research by Edmond Becquerel in 1839 [11], gained significant attention in the late 1960s, thanks to pioneers like Boddy [12] and Honda and Fujishima [13]. In their experiments, Honda and Fujishima coated a titanium dioxide (TiO_2) electrode with a thin film of platinum (Pt) and immersed it in a solution containing water. Upon subjecting the electrode to ultraviolet (UV) light, they observed the generation of oxygen gas at the anode and hydrogen gas at the cathode. This observation suggests that water is undergoing a photoelectrochemical process, resulting in the separation of its constituent elements ($H_2O \rightarrow H_2 + 1/2O_2$). The aforementioned discovery exemplified the potential of semiconductor materials, particularly TiO_2,

in serving as photocatalysts for the process of water splitting and the subsequent generation of renewable hydrogen. The phenomenon was designated as the "Honda–Fujishima effect" and served as the basis for extensive investigation in the field of photocatalysis.

Semiconductor photocatalysis focuses on the use of semiconductor materials as catalysts for light-driven chemical reactions. Semiconductor materials, namely, TiO_2, ZnO, and WO_3, exhibit unique properties that make them well-suited for usage in photocatalytic applications. The material absorbs photons of light and subsequently generates electron–hole pairs. When the energy of incident light equals or exceeds the bandgap energy of a material, electrons in the valence band (VB) are excited to the conduction band (CB), leaving behind positively charged holes in the VB (Figure 1.1b). The electrons and holes generated by photosensitivity have the ability to engage in diverse chemical reactions on the semiconductor's surface [5, 6, 14]. Semiconductor photocatalysts have the ability to facilitate various reactions, including water splitting, pollutant degradation, carbon dioxide reduction, and organic synthesis, by harnessing the energy from sunlight.

In the context of utilizing light energy for driving reactions, it is important to distinguish between two scenarios. First, there are situations where a material employs light energy to facilitate thermodynamically downhill reactions ($\Delta G < 0$, as depicted in Figure 1.1b). In this scenario, the material does not alter the thermodynamics of the reaction but rather enhances the reaction kinetics by providing an alternative pathway through the absorption of optical energy. In such cases, the material can be classified as a photocatalyst only if the photon is considered as a reactant. An example of this situation is the complete oxidation of phenol to CO_2 and H_2O ($\Delta G = -3027.36$ kJ mol^{-1}) [15]. Conversely, when a material utilizes light to drive thermodynamically uphill reactions (positive Gibbs free energy change, $\Delta G > 0$, as shown in Figure 1.1b), it can be considered as a form of photosynthesis. In this case, the material can be referred to as a "photocatalyst" if the photon is considered as one of the reactants. This is commonly observed in processes like water splitting and CO_2 reduction [16, 17], where the input of light energy enables these reactions to occur.

The process of photocatalysis on semiconductor materials involves a sequence or a series of steps that take place upon light irradiation. The aforementioned steps can be broadly classified as light absorption, charge generation, charge separation and recombination, reactant adsorption and product desorption, and surface catalytic reactions [18]. These steps, represented schematically in Figure 1.2a, collectively drive the photocatalytic process on a typical semiconductor material.

As mentioned above, a semiconductor material possesses a bandgap, which represents the difference in energy levels between the VB, where electrons are normally located, and the CB, where electrons can move freely. When a semiconductor is subjected to light with energy that is equivalent to or surpasses its bandgap, the

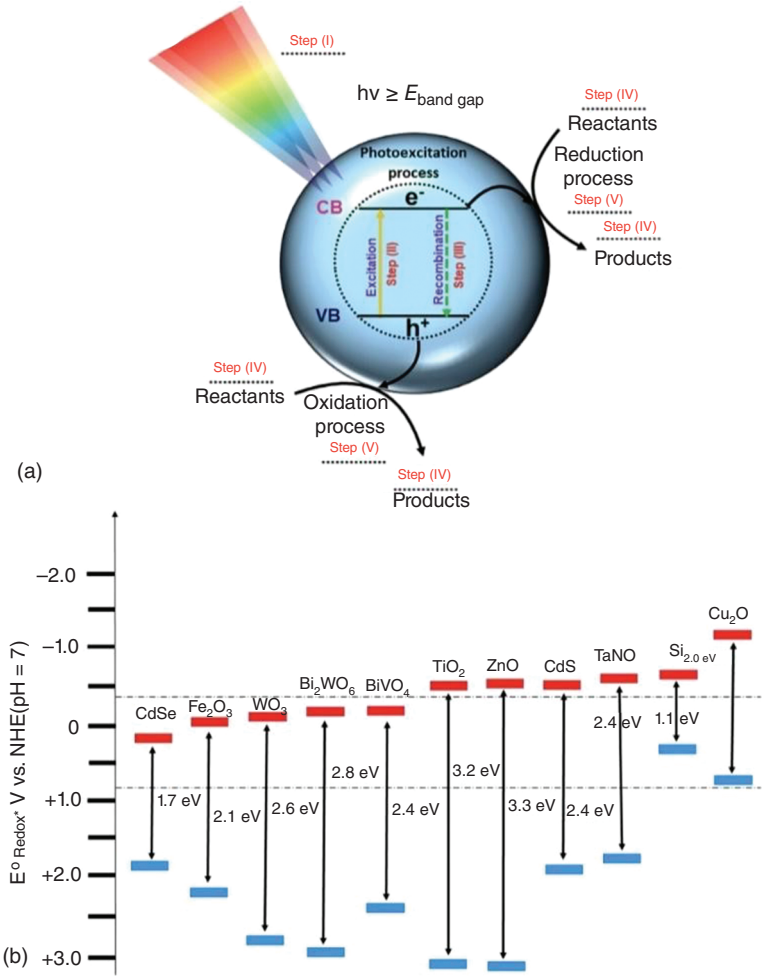

Figure 1.2 (a) Schematic representation of photocatalytic process. Source: Gouveia et al. [19]/Frontier Research Today/CC BY 4.0. (b) Schematic illustration of VB and CB potentials as well as the band gap energies of various semiconductor photocatalysts. Source: Reproduced with permission Xie et al. [20]/The Royal Society of Chemistry.

material absorbs photons. The process of absorption involves the excitation of electrons from the VB to the CB, leaving behind positively charged holes in the VB. This process results in the creation of electron–hole pairs within the semiconductor material. The term "excitons" is used to refer to the electron–hole pairs.

Charge separation is a critical process in photocatalytic reactions, wherein the photogenerated electrons and holes, possessing opposite charges, must be effectively separated to engage in distinct reactions. The phenomenon of separation is a result of the presence of an internal electric field within the semiconductor material.

However, there is also a chance that the electrons and holes recombine and lose their energy as heat. The phenomenon of charge separation plays a crucial role in facilitating efficient photocatalysis by impeding the recombination of electron–hole pairs [19, 21].

Following the separation of photogenerated electrons and holes, these charge carriers have the ability to engage in surface reactions occurring on the semiconductor material's surface. These reactions may encompass the participation of adsorbed reactants, such as water or organic compounds. In the process of water splitting, the photogenerated holes have the ability to undergo oxidation reactions with water molecules, resulting in the production of O_2 gas. Simultaneously, the photogenerated electrons possess the capability to engage in reduction reactions with protons, ultimately leading to the generation of H_2 gas. In the context of organic pollutant degradation, it is observed that semiconductor photocatalysis frequently encompasses the production of reactive oxygen species (ROS), namely hydroxyl radicals ($^{\bullet}OH$), superoxide ions ($^{\bullet}O_2^-$), and singlet oxygen ($^1O_2$), which are generated via reactions involving the photoinduced electrons and holes and water or oxygen molecules. ROS have the ability to engage in chemical reactions with organic compounds, resulting in the decomposition of these compounds into nontoxic substances [22].

Understanding and controlling these steps is essential for improving the efficiency of photocatalytic reactions. The primary area of interest for researchers lies in the enhancement of electron–hole separation efficiency and minimizing the recombination rates to achieve the high catalytic activity. Through a deeper understanding of these fundamental processes, we may advance the progress and utilization of photocatalysis in various fields, including but not limited to solar energy conversion, environmental remediation, and sustainable chemical synthesis.

1.3 Factors Affecting Photocatalytic Performance

Several factors, including light absorption efficiency and charge carrier separation and transfer, significantly impact the performance of photocatalysis. By carefully considering and optimizing these factors, researchers can improve the performance of photocatalytic systems, leading to efficient and effective photocatalytic processes.

1.3.1 Light Absorption

Generally, the energy available for the photocatalytic reaction is directly influenced by both the intensity and spectrum of the light source. Higher light intensity typically results in increased reaction rates, whereas the spectral match between the light source and the absorption properties of the photocatalyst governs the efficiency of light absorption. The choice of semiconductor material is fundamental as it determines the light absorption properties, bandgap energy, and electronic structure. Different materials have varying abilities to absorb specific wavelengths of light, which directly affects the efficiency of the photocatalytic reaction. The bandgap

energy of the semiconductor material dictates the minimum energy of photons required for electron excitation, and a suitable bandgap allows for the effective utilization of solar radiation. Narrow bandgap materials can absorb a broader range of light, including visible and near-infrared regions, while wide bandgap materials are more effective for UV light absorption (Figure 1.2b). UV radiation constitutes a minor fraction, specifically less than 4%, of the entire solar spectrum. In contrast, a significant portion, amounting to 43%, of the solar energy is concentrated within the visible light region. One of the primary objectives in scientific research is to identify a photocatalyst that exhibits two crucial features: its ability to effectively absorb visible light and a CB position that is suitably elevated. The absorption of visible light enables the utilization of a broader range of the solar spectrum, thereby enhancing the efficiency of the photocatalytic process. Also, in practical applications, it is commonly observed that the energy demand for the photocatalytic process exceeds the theoretical energy requirement for the generation of the desired products. Therefore, the presence of a high CB position is crucial in order to facilitate the requisite overpotential necessary for effective charge carrier transport and the promotion of desired chemical reactions.

Several strategies have been employed by researchers to enhance the absorption capacity of semiconductor photocatalysts, with a particular focus on visible light. One approach entails the introduction of dopant elements into a photocatalyst with a wide band gap, thereby sensitizing it and facilitating absorption within the range of visible light by influencing its electronic structure. Extensive research has been conducted on the utilization of metal ions, including Na^{+}, Zn^{2+}, Cu^{2+}, Fe^{3+}, Zr^{4+}, and W^{6+}, as well as nonmetal ions such as C, N, F, S, P, O, and B, as a means to reduce the bandgap and facilitate visible light absorption [23–25].

1.3.1.1 Metal/Nonmetal Doping

Metal ion doping has been shown to be an effective approach to boost the photocatalytic production of H_2. For instance, undoped ZnS nanoframes exhibited a lower photocatalytic H_2 production rate due to their limited ability to harvest visible light effectively [26]. However, the optimum doping of Cu^{2+} ions resulted in significant improvements in the photocatalytic efficiency of ZnS under visible light irradiation. The introduction of Cu ions created intermediate energy levels, allowing for effective charge separation and migration. On the other hand, the undoped $CuWO_4$ photocatalyst with a band gap of 2.46 eV demonstrated insufficient capacity to produce H_2 from water due to its CB potential of 0.23 V [27]. Nonetheless, doping V^{5+} ions into $CuWO_4$ resulted in a negative CB potential value of −0.11 V, favoring the production of H_2. These results emphasize the critical role of metal ion doping in improving photocatalytic performance and unlocking their potential for efficient H_2 generation.

Extensive research has focused on metal ions doping into photocatalysts; however, a limitation associated with metal ion doping is their susceptibility to photo-corrosion and potential recombination centers. These factors have the potential to impede the overall efficiency of the photocatalytic process. In order to address these challenges, nonmetal doping has emerged as an alternative strategy to

enhance photocatalytic performance. Nonmetallic dopants offer several advantages, including enhanced photostability, lower cost, and the absence of secondary pollutant effects. These dopants have shown promising results in improving the activity and stability of photocatalysts, rendering them a highly advantageous option for improving photocatalytic processes. For instance, the incorporation of C atoms into the TiO_2 structure has been found to result in a reduction in the band gap, leading to enhanced absorption of visible light. C-doped TiO_2 photocatalysts have been used for the degradation of organic compounds, such as dyes and pharmaceuticals, from aqueous matrices [28, 29].

The incorporation of C atoms into TiO_2 structure has been found to result in a reduction in the band gap, leading to enhanced absorption of visible light. C-doped TiO_2 photocatalysts have been used for the degradation of organic compounds, such as dyes and pharmaceuticals, from aqueous matrices [28, 29]. It has been suggested that the introduction of C atoms into TiO_2 creates a new impurity energy level located above the VB, resulting in a reduction of the band gap. This band gap narrowing allows the photocatalyst to absorb visible light, which was previously inaccessible. Upon light irradiation, electrons are directly promoted from the impurity level to the CB, generating electron–hole pairs (Figure 1.3a). The electrons participate in the reduction of O_2 molecules, leading to the formation of $O_2^{\bullet-}$ radicals. Simultaneously, the holes oxidize hydroxyl ions (OH^-) and H_2O, resulting in the production of $^{\bullet}OH$ radicals [32].

1.3.1.2 Plasmonic Photocatalysts

In recent years, there has been a growing interest in plasmonic photocatalysts for highly efficient photocatalysis processes [30, 33, 34]. These photocatalysts utilize nanoparticles (NPs) of noble metals such as Au, Ag, and Pt, which exhibit strong absorption in the UV–visible region due to a phenomenon called surface plasmon resonance (SPR). SPR refers to the collective oscillations of CB electrons in metal NPs induced by the electromagnetic field of incident light (Figure 1.3b) [30]. Localized surface plasmon resonance (LSPR) is an alternative term used to describe the phenomenon of surface plasmons. Plasmonic photocatalysts offer enhanced light absorption and field localization effects, enabling efficient generation and utilization of hot electrons and localized electromagnetic fields for improved photocatalytic activity. The resonance frequency of noble metal NPs, such as Au, Pt, and Ag, can be modulated by altering their size, shape, and local environment. This enables the adjustment of the resonance frequency to fall within the visible or near UV range. When the resonance frequency falls within the visible light range, it enables large bandgap photocatalysts like TiO_2 to become responsive to visible light. For low-bandgap photocatalysts, the SPR effect can considerably enhance the absorption of both visible and UV light, which is particularly beneficial for weakly absorbing materials.

For instance, a plasmonic-semiconductor structure consisting of Au nanoparticles (NPs) decorated TiO_2 nanotube arrays (TNTs), referred to as Au-TNTs, has been

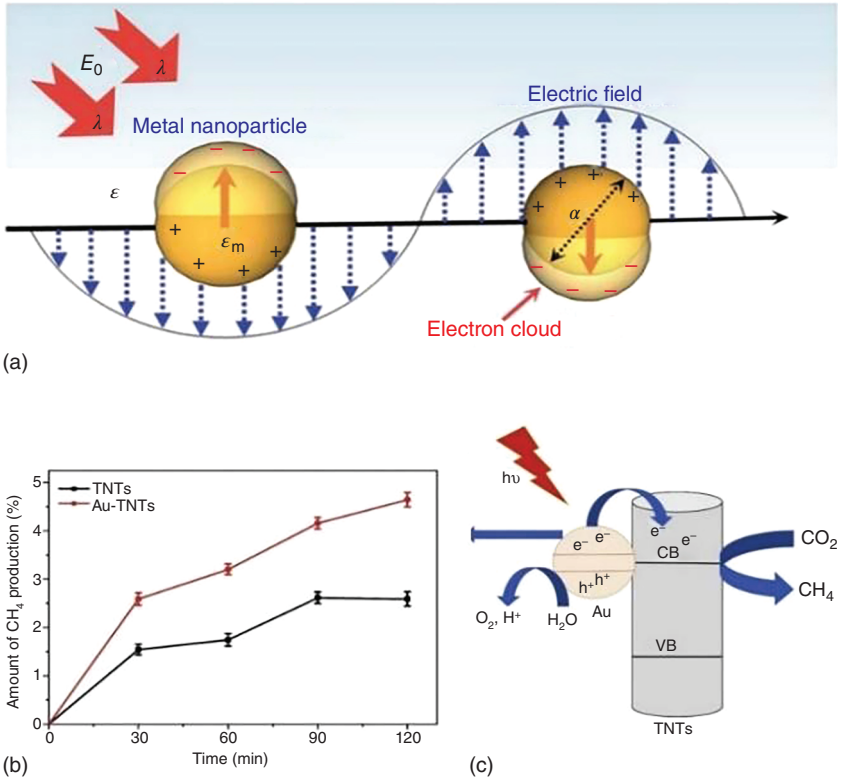

Figure 1.3 (a) Schematic illustration of the coherent oscillation of CB electrons induced by the interaction of light with plasmonic metal NPs. Source: Reproduced with permission Chou and Chen [30]/The Royal Society of Chemistry. (b) Amount of CH_4 production over TNTs and Au-TNTs photocatalysts over time. (c) Proposed mechanism of Au-TNTs photocatalyst for CO_2 reduction to CH_4 under visible light irradiation. Source: Reproduced with permission Khatun et al. [31]/Elsevier.

demonstrated as an effective photocatalyst for CO_2 reduction with water vapor under visible light irradiation [31]. The major carbon-containing product from this CO_2 reduction is CH_4. Figure 1.3b illustrates the time-dependent increase in CH_4 formation within the visible light range. The Au-TNTs photocatalyst exhibited higher photocatalytic activity for CH_4 production compared to pristine TNTs, indicating the significance of plasmonic Au NPs on TNTs in photocatalytic CO_2 reduction under visible light irradiation. As shown in Figure 1.3c, the enhancement of photocatalytic CO_2 reduction under visible light with Au-TNTs is attributed to the LSPR behavior of Au that could function with the TNTs as a visible light photocatalyst sensitizer. In addition, the hot electron generated on Au NPs move to the near CB of TiO_2, effectively activating the CO_2 reduction process. Through a series of subsequent reaction steps, this activation leads to the production of CH_4.

1.3.2 Charge Carrier Separation and Transfer

In photocatalysis, the efficient separation and transfer of generated charge carriers play a critical role in determining the overall photocatalytic performance [35]. Once generated, the charge carriers must be separated and transferred to the reaction sites on the photocatalyst surface to drive the redox reactions that convert reactants, such as water and CO_2, into valuable products like hydrogen, methanol, or other organic compounds. For example, in water splitting, the electrons are involved in the hydrogen evolution reaction, whereas the holes are utilized for the oxygen evolution reaction. Photogeneration of charges is the initial and fastest step in photocatalysis, occurring within femtoseconds (fs) upon light absorption. The separation and transport processes occur within picoseconds (ps) and microseconds (μs), depending on the material and its structural features. Thus, photogenerated charge carriers can rapidly transport to the surface reaction sites, where they participate in the desired redox reactions (over milliseconds to seconds). However, as time elapses from picoseconds to microseconds, some photogenerated charge carriers may recombine (picoseconds to microseconds), leading to the dissipation of their energy without participating in any chemical reaction (Figure 1.4a) [36]. Therefore, understanding and optimizing the charge carrier separation and transfer processes are crucial for enhancing the efficiency and selectivity of photocatalytic reactions.

From a physics perspective, the separation of photogenerated charges in photocatalysis can occur through various driving forces, such as a built-in electric field, diffusion, and trapping mechanisms [37]. The built-in electric field is considered the most common driving force for charge separation and forms the basis for typical strategies that have been developed in photocatalysis [36]. The built-in electric field in a photocatalytic system has two main origins. First, it arises from the spatial variation of space–charge concentrations, resulting from the presence of extrinsic dopants or electronic point defects within the bulk of the photocatalyst. Second, it can also be generated by the spatially varying charge density of surface sites on a nearly intrinsic photocatalyst. The difference in electrochemical potentials of the majority charge carriers between the reductive and oxidative sites creates an intrinsic asymmetry, leading to the establishment of the internal electric field. This phenomenon is exemplified in different photocatalytic structures, including solid-solid junctions (Figure 1.4b), metal oxide cocatalysts (Figure 1.4c), and crystal facet engineering (Figure 1.4d). The built-in electric field plays a critical role in guiding the direction of charge migration, minimizing recombination, and facilitating the desired redox reactions, ultimately leading to efficient light energy utilization in photocatalytic processes [38–41].

1.3.2.1 Solid–Solid Junctions

The creation of heterojunctions by combining two semiconductors has proven to be an efficient approach for achieving the spatial separation of photoexcited electron–hole pairs. When the two semiconductors possess different Fermi energy (EF) levels or work functions (W), a built-in electric field is spontaneously

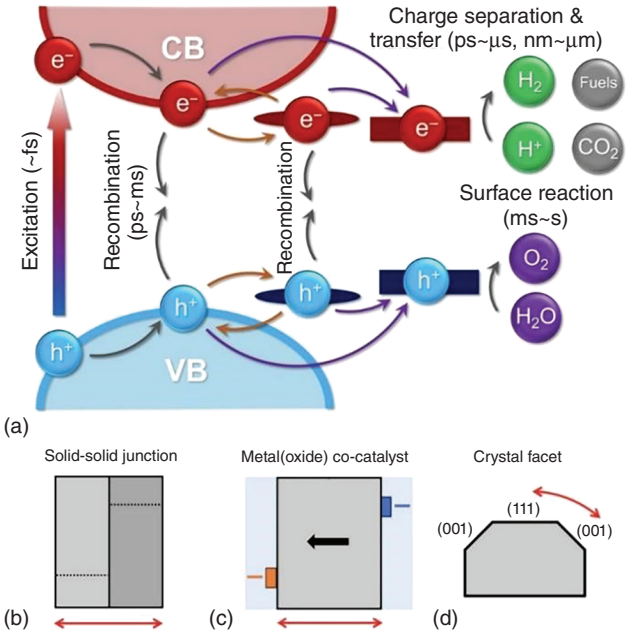

Figure 1.4 (a) Schematic illustration of the photocatalytic processes over a time span of femtoseconds to seconds. Source: Reproduced with permission from Chen et al. [36]/John Wiley & Sons. (b–d) Various strategies for achieving charge carriers separation. Blue and orange rectangles indicate reductive and oxidative sites, respectively. The red arrow indicates the charge-separation direction between the two surface sites. The solid arrow in panel (c) indicates internal electric fields. Source: Reproduced with permission from Liu et al. [37]/American Chemical Society.

formed at the heterojunction interface due to the diffusion of electrons from the semiconductor with a higher Fermi level to the one with lower Fermi level. When illuminated with light, photoexcited electrons and holes are compelled to move between the two semiconductors through the built-in electric field, effectively suppressing the recombination of the carriers. For the solid–solid junctions, two commonly encountered heterojunction types are the type II and Z-scheme. In a type II heterojunction (Figure 1.5a), the CB edge of semiconductor A is higher than that of semiconductor B, resulting in the transfer of photogenerated electrons from the CB of semiconductor A to that of semiconductor B. On the other hand, the VB edge of semiconductor A is higher than that of semiconductor B, causing photogenerated holes to move from the VB of semiconductor B to that of semiconductor A. This leads to efficient spatial charge separation. However, the type II heterojunction has a drawback, as the reductive and oxidative abilities of photogenerated electrons and holes are compromised due to the interfacial charge transfer. In contrast, the Z-scheme heterojunction (Figure 1.5b) also exhibits staggered energy band positions but maintains the redox abilities of photogenerated charges. In this arrangement, electrons in the CB of semiconductor B recombine

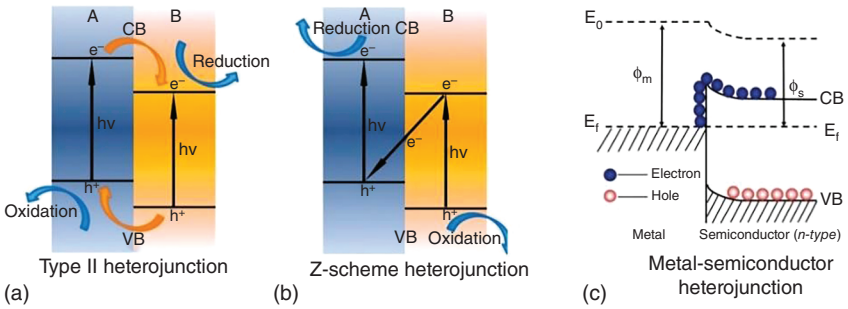

Figure 1.5 Band alignment in (a) type II heterojunction, (b) Z-scheme heterojunction. Source: Sun et al. [42]/John Wiley & Sons/CC BY 4.0. (c) Schematic of the Schottky barrier. Source: Reproduced with permission from Wang et al. [43]/Royal Society of Chemistry.

with the holes in the VB of semiconductor A, maintaining their respective reductive and oxidative capabilities. This unique characteristic of the Z-scheme heterojunction contributes to the efficient utilization of photogenerated charges in the photocatalytic process [42, 44]. An alternative effective approach for creating a space–charge separation region, known as the Schottky barrier, is by forming a metal–semiconductor junction. At the interface of the two materials, electrons move from one material to the other, aligning their EF levels. A common example is the heterojunction between an n-type semiconductor and a metal, where, ideally, the metal's work function is higher than that of the n-type semiconductor. Consequently, electrons flow from the semiconductor into the metal to adjust the Fermi energy levels (Figure 1.5c). The formation of the Schottky barrier results in an excess of negative charges on the metal and an excess of positive charges on the semiconductor [45]. Moreover, the Schottky barrier effectively acts as an electron trap, preventing electron–hole recombination in photocatalysis, thereby leading to enhanced photocatalytic performance [43].

1.3.2.2 Facet Engineering

Crystal facets have been extensively employed to induce charge transfer within semiconductor photocatalysts. By exposing various crystal facets, spatially varying band edge positions are formed, leading to varying surface charge densities. This variation in charge density establishes an electric field that drives the transport of charge carriers, contributing to enhanced charge separation and migration within the photocatalyst. Recent studies have reported accelerated charge separation and enhanced quantum efficiency at the interface of {001}/{101} co-exposed facets in shape-tailored TiO_2 crystals [46]. This phenomenon is likely attributed to the generation of an internal electric field resulting from the band alignment difference between the two exposed facets. The constructed {001}/{101} facet junction, which enables effective carrier separation between different exposed facets, demonstrates a remarkable increase in quantum efficiency and catalytic performance in hydrogen evolution reaction compared to TiO_2 polycrystals [40].

1.3.2.3 Cocatalyst Loading

Cocatalyst loading is an effective strategy to enhance the photocatalytic activity of semiconductor photocatalysts [47]. This approach improves the efficiency of charge separation and enhances the number of exposed active sites. Recently, tailoring the attachment of cocatalysts to specific facets has garnered significant attention in the field of photocatalytic applications. For example, in $SrTiO_3$ photocatalysts, a selective attachment of H_2-evolving cocatalysts and water-oxidation cocatalysts onto both reductive and oxidative facets was demonstrated to result in a remarkable fivefold enhancement of quantum yield (QY) [48]. This strategic approach resulted in an impressive approximately 100% QY on $SrTiO_3$ particles [39]. Li et al. reported a selective photodeposition of MnO_x cocatalysts onto the {011} facets of a single $BiVO_4$ photocatalyst in an asymmetric manner. The deposition of the cocatalyst resulted in a significant enhancement in the photocatalytic activity of water oxidation [49]. Spatially resolved surface photovoltage (SRSPV) technique was used to understand the function of the cocatalyst and the underlying mechanism [50]. Impressively, the SRSPV analysis revealed that the selective deposition of cocatalysts facilitated the efficient spatial separation of photogenerated holes and electrons, effectively distributing them at the lateral {011} and top {010} facets, respectively, as depicted in Figure 1.6a. The SRSPV spectra provided quantitative evidence of the asymmetric deposition's effects, showing a significant enhancement in positive surface photovoltage (SPV) signals on the {011} facets, whereas the SPV signals on the {010} facets exhibited an inverted sign (Figure 1.6b). This observed change indicated aa shift in the vectors of the built-in electric fields on the different facets, transitioning from counteraction to alignment. Consequently, photogenerated holes and electrons were efficiently separated between the {011} and {010} facets due to the aligned built-in electric field (Figure 1.6c). Further selective deposition of Pt NPs onto the {010} facets increased the surface photovoltage signals on both facets with opposite signs, indicating enhanced hole transfer to the {011} facets and electron transfer to the {010} facets. The asymmetric assembly of cocatalysts resulted in a substantial 2.5 kV cm^{-1} built-in electric field, oriented from the {010} facet to the {011} facet, facilitating efficient charge separation.

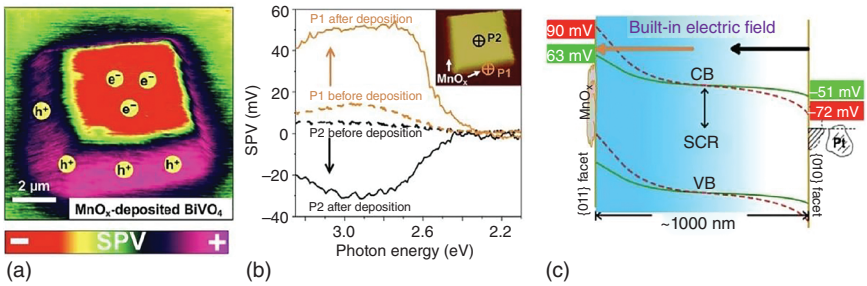

Figure 1.6 Charge separation through a spatially selective cocatalyst loading, (a) Surface photovoltage microscopy (SPVM) analysis, (b) Spatially resolved surface photovoltage (SRSPS) analysis, and (c) schematic illustration of the charge separation process.
Source: Reproduced with permission from Chen et al. [36]/John Wiley & Sons.

1.4 Investigation of Photocatalysis for Real Applications

Over the years, photocatalysis technology has witnessed significant advancements and holds great promise for various applications. As the photocatalysis technology matures, there is an increasing emphasis on scaling up production processes and developing practical applications. Strategies to overcome challenges related to catalyst stability, reactor design, and large-scale synthesis are being explored to enable the industrial implementation of photocatalytic processes. Researchers are continuously striving to replicate real or quasi-real conditions in their experiments to test the applicability of new materials. Before any material can be utilized in commercial applications, it must undergo rigorous testing. For instance, in the case of NO_x abatement, Chen et al. [51] conducted investigations on photocatalytic coating elements applied to road pavements. They tested a cement concrete slab incorporated with a TiO_2 photocatalyst under artificial daylight irradiation, simulating real-world conditions. The results showed an impressive conversion rate of over 90% for NO through the photooxidation process. The researchers also studied the impact of inlet NO concentration on the efficiency of NO_x removal, and they found high removal efficiency for residence times ranging from 5 to 20 minutes.

Photocatalysis for NO_x removal has not only been studied in pilot-scale reactors but also been implemented in real commercial objects, particularly building materials. For example, Guerrini and Corazza [52] reported the first application of cement containing TiO_2 in 1996 in the construction of the symbolic sails of the "Dives in Misericordia" Church in Rome, Italy (Figure 1.7). This real-world application

Figure 1.7 In Misericordia Church, Rome, constructed of TiO_2 self-cleaning and depolluting TX Active cement (inaugurated in 2003). Source: Serpone [53]/MDPI/CC BY 4.0.

showcases the practicality and potential of using photocatalytic materials for air pollution control in large-scale structures and demonstrates the progress in incorporating this technology into commercial settings.

Recently, there has been a growing focus on converting solar energy into chemicals. Various technologies, such as photovoltaic-assisted electrochemical, photoelectrochemical, and photocatalytic water splitting systems, have been developed to produce solar hydrogen from water. Among these, photovoltaic-assisted electrolyzers have shown great promise, achieving efficiencies as high as 30%. By combining these systems with fuel cells, end-users can generate both solar power and solar fuels, ensuring continuous energy supply throughout the year on a regional scale. Although particulate photocatalyst systems have generally shown lower solar-to-hydrogen (STH) values, typically around 1% at most, ongoing research focuses on enhancing photocatalyst performance. The goal is to make these systems more viable, benefiting from their simplicity and scalability. However, it is essential to address the safe and efficient handling of product gases to ensure practical implementation. As photocatalysis technology continues to advance, it holds the potential to revolutionize solar energy conversion and fuel production, contributing to a more sustainable and environmentally friendly energy landscape.

To explore the scalability and gas handling of solar hydrogen production through photocatalytic water splitting, Domen and coworkers [54, 55] have developed panel reactors utilizing photocatalyst sheets, as depicted in Figure 1.8. At the Kakioka Research Facility within the University of Tokyo, they constructed a 100-m^2 scale prototype photocatalytic solar hydrogen production system consisting of 1600 reactor units. Each unit is equipped with a light-receiving area of 625 cm^2, and the gap between the UV-transparent glass window and the photocatalyst sheet is precisely adjusted to 0.1 mm. This adjustment minimizes the water load, prevents the accumulation and ignition of the product oxyhydrogen gas, and ensures the safe operation of the system.

During field tests conducted over a specific time span, an STH efficiency of 0.76% was obtained under natural sunlight irradiation on a summer day (a solar irradiance of 0.88 $kW\,m^{-1}$). Lately, continuous data collection of solar irradiance and photocatalytic H_2 and O_2 production and the STH efficiency showed a slight decrease from 0.5% to 0.2%, which corresponded to the decline in the proportion of UV light in natural sunlight from 5% to 2%. This indicated that the photocatalyst's performance was well-maintained during the trial. By linking the solar water splitting and gas separation units, a filtrate gas with approximately 94% H_2 content was obtained. The H_2 concentration was close to the range outside the explosion limit, ensuring safety during gas handling. While this preliminary assessment indicated that the solar hydrogen production system presented a very low risk, further in-depth hazard analysis is necessary. These pioneering achievements provide a successful construction and operation of a large-scale solar hydrogen production system.

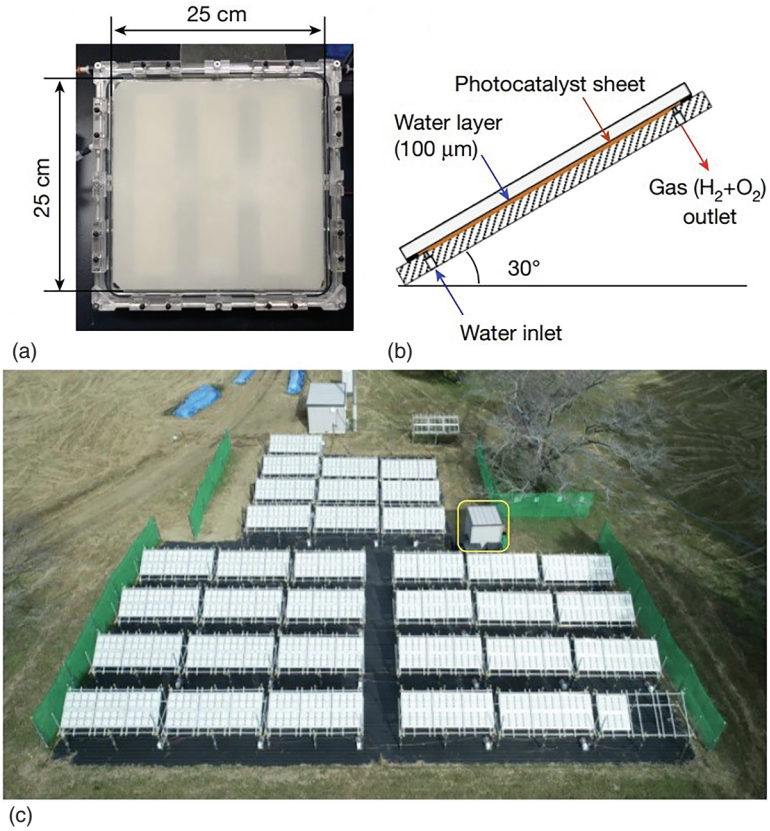

Figure 1.8 The 100-m^2 water splitting photocatalyst panel reactor, (a) A photographic image of a panel reactor unit (625 cm^2). (b) The structure of the panel reactor unit viewed from the side. (c) An overhead view of the 100-m^2 solar hydrogen production system consisting of 1600 panel reactor units and a hut housing a gas separation facility (indicated by the yellow box). Source: Reproduced with permission from Nishiyama et al. [55]/Springer Nature.

1.5 Conclusion

Photocatalysis has found numerous applications in various fields due to its ability to harness solar energy and drive chemical reactions. Researchers are continuously exploring novel materials and improving existing ones to enhance photocatalytic efficiency. Efforts are focused on designing materials with tailored properties, optimal band structures, and efficient charge separation, leading to higher QYs and faster reaction rates. The trend is shifting toward the development of visible light-responsive photocatalysts. Strategies such as doping, cocatalyst deposition, heterojunctions, and crystal facet engineering are employed to extend light absorption into the visible spectrum as well as to improve charge transfer efficiency, thereby increasing the overall photocatalytic performance.

By conducting thorough investigations that encompass various aspects such as scale-up studies and cost–benefit analysis, researchers can gain a comprehensive understanding of the real-world potential of photocatalysis and explore its practical applications in diverse fields, including water purification, air pollution control, self-cleaning surfaces, and renewable energy generation. Although significant progress has been made in solar-to-fuel conversion technologies, there remains a critical need to substantially enhance the current solar-to-fuel conversion efficiency, which hovers around approximately 1%. To achieve meaningful and widespread impact on solar fuels production, the efficiency must be raised to exceed 10%. This enhancement is essential for scaling up the technology and making it a practical and viable solution for sustainable energy production from solar sources. Continued research, development, and innovation are vital to address this challenge and unlock the full potential of solar fuels as a clean and renewable energy source.

References

1 N. Armaroliand V. Balzani. (2016) Chemistry A *European Journal,* 22, 32.
2 Shaner, M.R., Atwater, H.A., Lewis, N.S. et al. (2016). *Energy & Environmental Science* 9: 2354.
3 Serpone, N. and Pelizzetti, E. (1989). *Photocatalysis: Fundamentals and Applications*. New York: Wiley.
4 Liu, B., Zhao, X., Yu, J. et al. (2019). *Journal of Photochemistry and Photobiology C: Photochemistry Reviews* 39: 1.
5 Schneider, J., Matsuoka, M., Takeuchi, M. et al. (2014). *Chemical Reviews* 114: 9919.
6 Sun, X., Huang, H., Zhao, Q. et al. (2020). *Advanced Functional Materials* 30: 1910005.
7 Berardi, S., Drouet, S., Francas, L. et al. (2014). *Chemical Society Reviews* 43: 7501.
8 Yang, X. and Wang, D. (2018). *ACS Applied Energy Materials* 1 (6657).
9 Tachibana, Y., Vayssieres, L., and Durrant, J.R. (2012). *Nature Photonics* 115: 199.
10 Liu, B., Wu, H., and Parkin, I.P. (2020). *ACS Omega* 5: 14847.
11 Becquerel, A.E. (1839). *Comptes rendus* 9: 561–567.
12 Boddy, P.J. (1986). *Journal of the Electrochemical Society* 115: 199.
13 Fujishima, A. and Honda, K. (1972). *Nature* 238: 37.
14 Linsebigler, A., Lu, G., and Yates, J.T. (1995). *Chemical Reviews* 95: 735.
15 Lide, D.R. (2003). *Journal of the American Chemical Society* 126: 1586.
16 Chen, S., Takata, T., and Domen, K. (2017). *Nature Reviews Materials* 2: 17050.
17 Chang, X.X., Wang, T., and Gong, J.L. (2016). *Energy & Environmental Science* 9: 2177.
18 Zhong, S., Xi, Y., Chen, Q. et al. (2020). *Nanoscale* 12: 5764.
19 Gouveia, A.F., Assis, M., and Laécio, S. (2018). *Frontier Research Today* 1: 1.

20 Xie, S., Zhang, Q., Liu, G., and Wang, Y. (2016). *Chemical Communications* 52: 35.
21 Xu, Q., Zhang, L., Yu, J. et al. (2018). *Materials Today* 21: 1042.
22 Hussain, C.M. and Nassar, N.N. (2023). *Nanoremediation*. Elsevier.
23 Suresh, R., Gnanasekaran, L., Rajendran, S., and Soto-Moscoso, M. (2023). *Fuel* 348: 128528.
24 Wang, Q., Rhimi, B., Wang, H., and Wang, C. (2020). *Applied Surface Science* 530: 147286.
25 Rhimi, B., Jouini, H., Padervand, M. et al. (2022). *Journal of Environmental Chemical Engineering* 10: 108566.
26 Huang, J., Chen, J., Liu, W. et al. (2022). *Chinese Journal of Catalysis* 43: 782.
27 Tri, N.L.M., Trung, D.Q., Thuan, D.V. et al. (2020). *Applied Surface Science* 45: 18186.
28 Matos, J., Miralles-Cuevas, S., Ruíz-Delgado, A. et al. (2017). *Carbon* 122: 361.
29 Chauhan, A., Sharma, M., Kumar, S. et al. (2020). *Journal of Hazardous Materials* 381: 120883.
30 Chou, C.-H. and Chen, F.-C. (2014). *Nanoscale* 6: 8444.
31 Khatun, F., Aziz, A.A., Sim, L.C., and Monir, M.U. (2019). *Journal of Environmental Chemical Engineering* 7: 103233.
32 Shao, J., Sheng, W., Wang, M. et al. (2017). *Applied Catalysis B: Environmental* 209: 311.
33 Aoki, Y., Ishida, T., and Tatsuma, T. (2022). *ACS Applied Nano Materials* 5: 4406.
34 Chen, Q. and Tan, Y. (2023). *Nano Research* 16: 5919.
35 Liu, B., Zhao, X., Parkin, I.P., and Nakata, K. (2020). *Interface Science and Technology* 31: 103.
36 Chen, R., Fan, F., and Li, C. (2022). *Angewandte Chemie (International Ed. in English)* 61: e202117567.
37 Yanagi, R., Zhao, T., Solanki, D. et al. (2022). *ACS Energy Letters* 7: 432.
38 Chen, F., Huang, H., Guo, L. et al. (2019). *Angewandte Chemie (International Ed. in English)* 58: 10061.
39 Takata, T., Jiang, J., Sakata, Y. et al. (2020). *Nature* 581: 411.
40 Zhang, A.-Y., Wang, W.-Y., Chen, J.-J. et al. (2018). *Energy and Environmental Science* 11: 1444.
41 Wang, D., Sheng, T., Chen, J. et al. (2018). *Nature Catalysis* 1: 291.
42 Sun, H., Dong, C., Liu, Q. et al. (2020). *Advanced Materials* 32: 2002486.
43 Wang, H., Zhang, L., Chen, Z. et al. (2014). *Chemical Society Reviews* 43: 5234.
44 Sun, S.D., He, L., Yang, M. et al. (2022). *Advanced Functional Materials* 32: 2106982.
45 Yang, H. (2021). *Materials Research Bulletin* 142: 111406.
46 Tachikawa, T., Yamashita, S., and Majima, T. (2011). *Journal of the American Chemical Society* 133: 7197.
47 Zhang, K., Ran, J., Zhu, B. et al. (2018). *Small* 14: e1801705.
48 Mu, L., Zhao, Y., Li, A. et al. (2016). *Energy and Environmental Science* 9: 2463.
49 Li, R., Zhang, F., Wang, D. et al. (2013). *Nature Communications* 4: 1432.
50 Zhu, J., Pang, S., Dittrich, T. et al. (2017). *Nano Letters* 17: 6735.

51 Chen, D.H., Li, K., and Yuan, R. (2007). Annual Project Report Submitted to Houston Advanced Research Center and Office of Air Quality Planning and Standards. U.S. Environmental Protection Agency. Research Triangle Park, pp. 1–17.
52 Guerrini, G.L. and Corazza, F. (2008). White cement and photocatalysis part 1: Fundamentals. *First Arab International Conference and Exhibition on the Uses of White Cement*. Cairo, Egypt, (28–30 April 2008).
53 Serpone, N. (2018). *Catalysts* 8: 553.
54 Yamada, T. and Domen, K. (2018). *ChemEngineering* 2: 36.
55 Nishiyama, H., Yamada, T., Nakabayashi, M. et al. (2021). *Nature* 598: 304.